Resonance in downhole microseismic data and its removal

Zhishuai Zhang, James W. Rector, and Michael J. Nava, University of California, Berkeley*

Summary

We identified resonance due to poor geophone-borehole coupling in downhole microseismic data and proposed to use spiking deconvolution and relative spectrum analysis to remove its effect. The resonance may hinder the arrival time picking and contaminate microseismic waveform spectrum. We designed a spiking deconvolution filter to recover the impulse response of the earth. Also, we proposed to use relative spectrum analysis to study microseismic source parameters. The application of deconvolution on Marcellus shale dataset improved the identifiability of the multiple arrivals. Additionally, the relative spectrum analysis is more effective in revealing the actual spectrum characteristics of microseismic waveforms.

Introduction

Microseismic location, magnitude, and source parameter estimations highly depend on signal quality (Eisner et al., 2009; Maxwell, 2010, 2014; Warpinski et al., 2009). Various factors, including recording-system factors and background noise, make the characterization of microseismic data a complex and challenging task. Among these factors, resonance due to the poor coupling of borehole geophones contributes significantly to waveform distortion (Gaiser et al., 1988; Maxwell, 2014; Nava et al., 2015; Zhang et al., 2015), but is often not treated properly.

Gaiser et al. (1988) studied the seismic response of a three-component geophone in a vertical borehole. The geophone was locked with a locking arm in the wellbore. The waveforms show that there is usually serious resonance in the direction perpendicular to the locking force. In downhole microseismic monitoring, this resonance is relatively common. The situation is even worse for geophones deployed in horizontal wells, where the only coupling force between geophones and wellbore is usually the gravitational force of the geophones (Nava et al., 2015; Zhang et al., 2015). In these situations, we usually cannot avoid the geophone resonance other than the axial component data.

Due to the limited azimuthal coverage of geophones in downhole microseismic acquisition, polarization directions of P-waves are usually used to constrain the microseismic event locations. However, the resonance issue usually leads to a significant error in polarization direction estimation (Zhang et al., 2015). This polarization direction uncertainty can be a major source of microseismic event location uncertainty in downhole monitoring. Multiple arrivals can be used to improve location accuracy in downhole microseismic survey (Pei et al., 2014; Zhang et al., 2015; Zimmer, 2011), however, the identification of some phases can be hindered by the resonance from their preceding phases. In addition, source parameters are useful for microseismic characterization (Cipolla et al., 2012; Du et al., 2011; Eisner et al., 2007; Rutledge and Phillips, 2003; Urbancic et al., 2002). The resonance issue is even more critical for these studies since the full waveform is usually required. A bandpass filter has been applied in previous research (Nava et al., 2015) to mitigate this artifact, however, this is based on the assumption that the resonance frequency is different from microseismic spectrum band and may result in signal loss otherwise.

The purpose of this work is to identify resonance due to poor geophone-borehole coupling and propose procedures to tackle this issue. With a microseismic survey in a single horizontal well in Marcellus shale, we found that both geophone components perpendicular to the axial direction are seriously affected by the coupling issue. With a carefully designed deconvolution filter, we are able to remove the source and receiver signatures, thus, successfully recover the impulse response of the earth, and makes the phase identification easier. We also bring up the importance of relative spectrum in frequency analysis since individual event spectrum may be significantly affected by receiver response of the geophones.

Theory and Method

We used spiking deconvolution to recover the impulse response of the earth. In terms of the analysis of the microseismic events, we proposed to study the relative spectrum to mitigate the artifact from resonance.

Resonance due to poor coupling

Gaiser et al. (1988) conducted a coupling response experiment to study the resonance of geophones under normal vertical seismic profile (VSP) conditions. The geophone was locked in the borehole with a horizontal locking force. They found the geophone was subject to severe resonance issues in the horizontal direction perpendicular to the locking force due to poor geophone-borehole coupling. Various downhole microseismic surveys have this problem as well.

In the cases where the geophones are deployed in horizontal wells, the situation is even worse since the only coupling force between the geophones and borehole is usually the gravitational force of the geophones. This, together with the unknown orientation of downhole geophone, makes the microseismic signal analysis extremely challenging.

Deconvolution of microseismic signal

Under the assumption that the impulse response of the earth is random, the seismogram has the same amplitude spectrum of the convolution of the source wavelet and the geophone response. An additional minimum phase assumption enables the determination of an optimum Wiener filter, which can recover the impulse response of the earth from the recorded seismogram (Yilmaz, 2001). This can be used to remove the source signature and geophone resonance, thus, improve the identifiability of the multiple arrivals.

Relative spectrum analysis

If the background noise is negligible, the recorded seismogram due to a microseismic event can be expressed as the convolu-

tion of source wavelet, path impulse response, and geophone response (including resonance due to poor coupling):

$$x(t) = w(t) * e(t) * r(t), \tag{1}$$

where $x(t)$ is the recorded seismogram, $w(t)$ is the source wavelet, $e(t)$ is the earth impulse response, and $r(t)$ is the receiver (geophone) response.

Its equivalent form in the Fourier domain is

$$X(\omega) = W(\omega)E(\omega)R(\omega), \tag{2}$$

where $X(\omega)$, $W(\omega)$, $E(\omega)$ and $R(\omega)$ are the Fourier domain representation of $x(t)$, $w(t)$, $e(t)$ and $r(t)$, respectively.

For any microseismic event with index i, the ratio between its waveforms in the Fourier domain and the average spectrum over all the N events recorded by the same geophone can be expressed as

$$\frac{X_i(\omega)}{\sum_{n=1}^{N} X_n(\omega)} = \frac{W_i(\omega)E_i(\omega)R(\omega)}{\sum_{n=1}^{N} W_n(\omega)E_n(\omega)R(\omega)} = \frac{W_i(\omega)E_i(\omega)}{\sum_{n=1}^{N} W_n(\omega)E_n(\omega)}. \tag{3}$$

Again, under the assumption that the impulse response of the earth is random, the Fourier representation $E_n(\omega)$ is white. So the relative spectrum of event i is approximately equal to

$$\frac{X_i(\omega)}{\sum_{n=1}^{N} X_n(\omega)} \approx \frac{W_i(\omega)}{\sum_{n=1}^{N} W_n(\omega)}. \tag{4}$$

This expression is not affected by the receiver response $R(\omega)$, so it is a better representation of the real spectrum of the microseismic event.

Microseismic Survey in Marcellus Shale

We studied the poor coupling problem in a microseismic dataset from the Marcellus shale. This project consists of two horizontal wells: the stimulation well and the monitor well (Figure 1). Microseismic locations have been estimated by a contractor shown in Figure 1 as well. The detailed information about this project has been given by Zhang et al. (2015).

There are four perforation shots prior to each stimulation stage in this hydraulic fracturing. As shown in Figure 2, the geophone array consists of eleven three-component geophones and was moved according to the stimulation zone to increase the S/N.

Results and Discussion

Figure 3 is a sample three-component waveform of a perforation shot in stage 6. There are strong resonances in all of the three components in this case, especially for component 1 as denoted in the figure. This is a common phenomenon for both microseismic event and perforation shot waveforms.

Deconvolution

We first performed a spiking deconvolution to remove the source and receiver signatures in these waveforms. An optimum Wiener

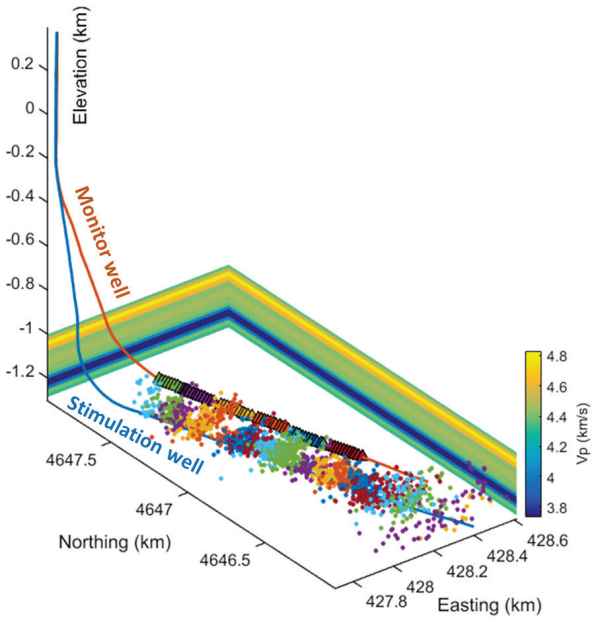

Figure 1: Hydraulic fracturing project overview. The microseismic events (dots) are colored according to their stimulation stages. The geophone arrays (triangles) are colored according to their locations.

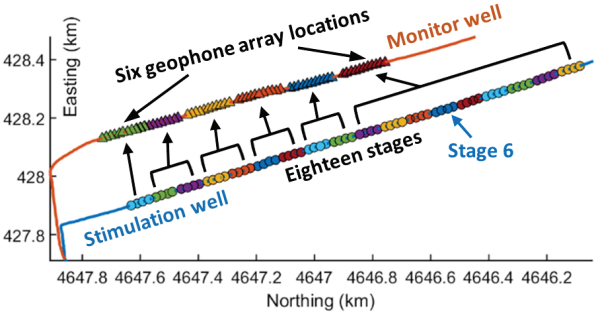

Figure 2: An array of eleven three-component geophones was used to monitor the stimulation. It was moved according to the stimulation zone locations to increase S/N.

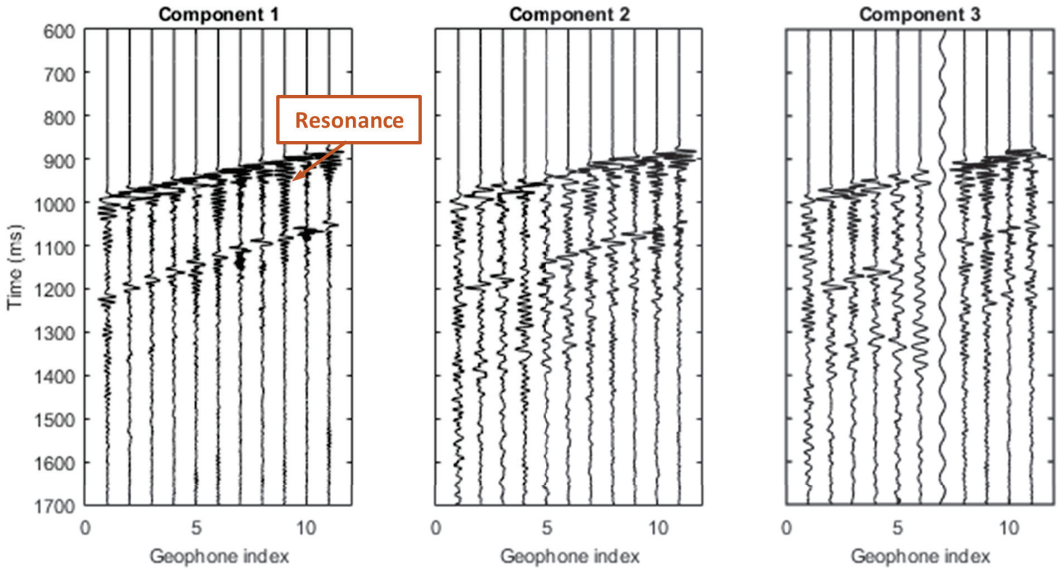

Figure 3: Sample three-component waveform of a perforation shot. All of the three components, especially component 1, show strong resonance after the P-wave and S-wave arrivals due to the poor geophone-borehole coupling.

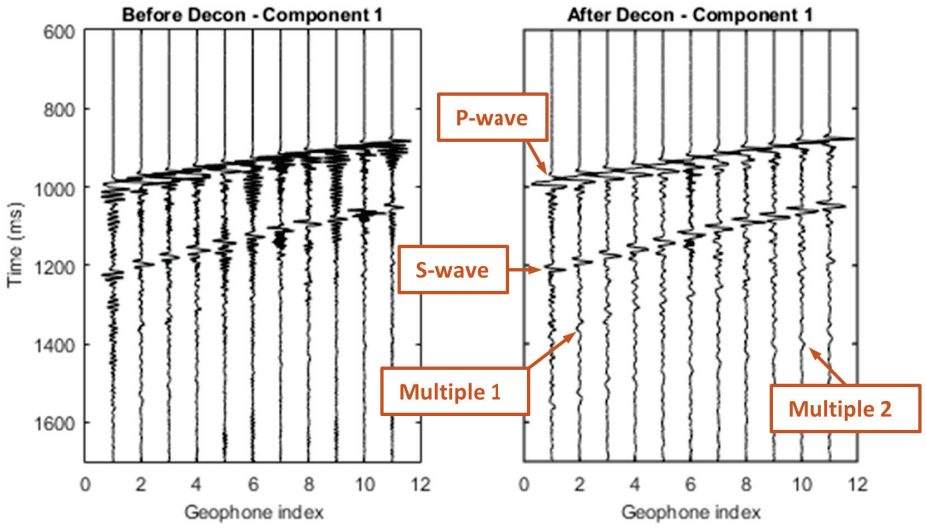

Figure 4: Deconvolution result of component 1. The deconvolution successfully suppressed the resonance in the original data. In addition, it brings up the multiple arrivals that are hardly identified in the original waveform.

filter was designed using the average autocorrelation of the four perforation shots in stage 6.

The deconvolution result is in Figure 4. From the comparison, we can see a significant suppression of the resonance after P- and S-wave arrivals by the deconvolution. This prevents the later phases from being contaminated by resonance due to earlier arrivals. For instance, it can be difficult to decide the S-wave arrival times on geophone 6 and 9 in Figure 4 due to their preceding resonance. However, after the removal of the resonance, it is much easier to pick those arrivals. In addition, we also find two weak, yet clear phases after the deconvolution denoted by multiple 1 and multiple 2 in Figure 4. These two arrivals can hardly be identified in the original data.

Relative spectrum analysis

Figure 5 shows the effect of relative spectrum analysis compared with single waveform spectrum analysis. Figures 5a and 5b show 52 single microseismic event spectra of P-wave and S-wave. The events are sorted according to the peak frequency of P-wave spectrum. However, we cannot see any effect of this sorting in the S-wave spectrum (Figures 5b).

Then, we normalized the P-wave and S-wave spectrum with their average over all these microseismic events. The result is shown in Figures 5c and 5d. Compared with the spectrum of single events, the relative S-wave spectrum shows a similar trend (Figures 5d) with that of P-wave after the events are sorted with peak P-wave spectrum. This shows that there is an intrinsic correlation between P-wave and S-wave spectrum of the same event. The spectrum of single microseismic event does not have this trend due to the effect geophone resonance. The relative spectrum analysis is able to reveal this correlation.

Conclusions

We discussed the issue of geophone resonance due to poor coupling in a microseismic survey. Severe resonance problem is identified in the downhole microseismic dataset from Marcellus shale. We designed a spiking deconvolution filter according to the waveforms. The deconvolution is successful in removing resonance and improves the identifiability of multiple arrivals. A relative spectrum analysis is proposed for microseismic source parameters study. The relative spectrum analysis is not affected by resonance issue and reveals the correlation between P-wave and S-wave spectrum for the same events.

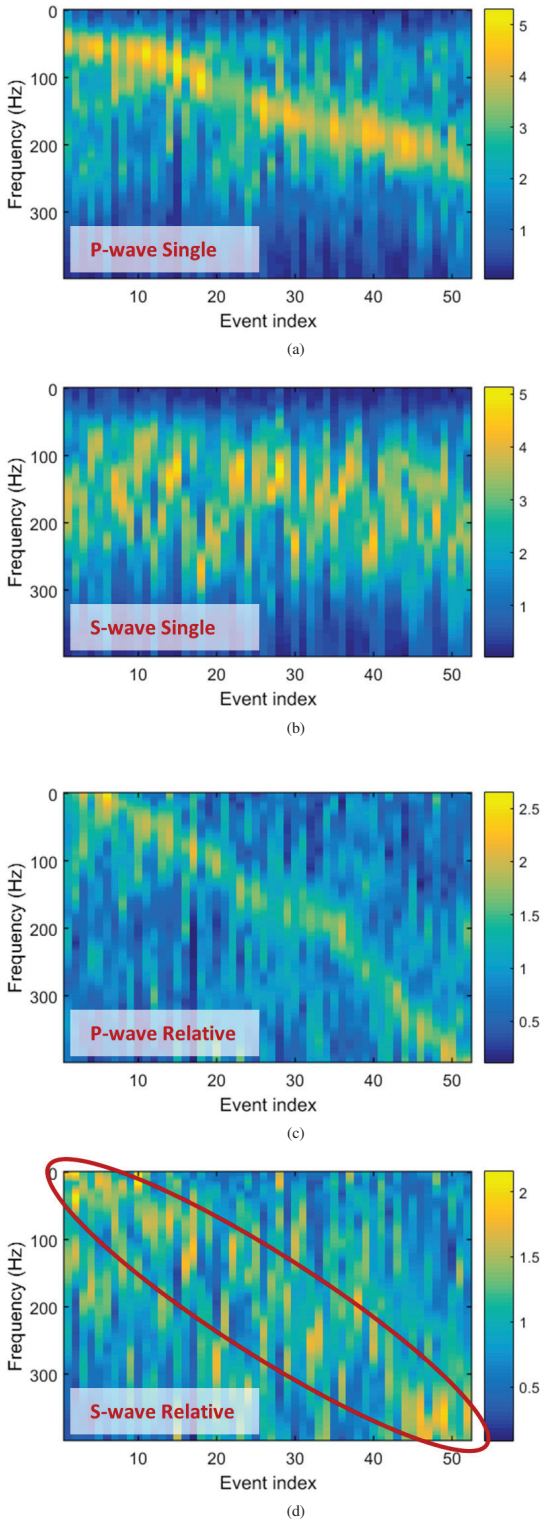

Figure 5: Single spectrum analysis (a and b) and relative spectrum analysis (c and d). The events are sorted according to the peak frequency of P-wave spectrum. The relative S-wave spectrum (d) shows a similar trend with P-wave spectrum (c). However, we cannot see this phenomenon from the single spectrum analysis.

EDITED REFERENCES

Note: This reference list is a copyedited version of the reference list submitted by the author. Reference lists for the 2016 SEG Technical Program Expanded Abstracts have been copyedited so that references provided with the online metadata for each paper will achieve a high degree of linking to cited sources that appear on the Web.

REFERENCES

Cipolla, C., S. Maxwell, M. Mack, and R. Downie, 2012, A practical guide to interpreting microseismic measurements: Presented at the SPE/EAGE European Unconventional Resources Conference and Exhibition-From Potential to Production.

Du, J., U. Zimmer, and N. Warpinski, 2011, Fault plane solutions from moment tensor inversion for microseismic events using single-well and multi-well data: Focus.

Eisner, L., P. M. Duncan, W. M. Heigl, and W. R. Keller, 2009, Uncertainties in passive seismic monitoring: The Leading Edge, **28**, 648–655, http://dx.doi.org/10.1190/1.3148403.

Eisner, L., and J. H. Le Calvez, 2007, New analytical techniques to help improve our understanding of hydraulically induced microseismicity and fracture propagation: Presented at the SPE Annual Technical Conference and Exhibition, SPE.

Gaiser, J. E., T. J. Fulp, S. G. Petermann, and G. M. Karner, 1988, Vertical seismic profile sonde coupling: Geophysics, **53**, 206–214, http://dx.doi.org/10.1190/1.1442456.

Maxwell, S., 2010, Microseismic: Growth born from success: The Leading Edge, **29**, 338–343, http://dx.doi.org/10.1190/1.3353732.

Maxwell, S., 2014, Microseismic imaging of hydraulic fracturing: Improved engineering of unconventional shale reservoirs: SEG Books.

Nava, M. J., J. W. Rector, and Z. Zhang, 2015, Characterization of microseismic source mechanism in the Marcellus shale through analysis in the spectral domain: 85th Annual International Meeting, SEG, Expanded Abstracts, http://dx.doi.org/10.1190/segam2015-5911950.1.

Pei, D., J. Carmichael, C. Waltman, and N. Warpinski, 2014, Microseismic anisotropic velocity calibration by using both direct and reflected arrivals: 84th Annual International Meeting, SEG, Expanded Abstracts, http://dx.doi.org/10.1190/segam2014-0097.1.

Rutledge, J. T., and W. S. Phillips, 2003, Hydraulic stimulation of natural fractures as revealed by induced microearthquakes, Carthage Cotton Valley gas field, east Texas: Geophysics, **68**, 441–452, http://dx.doi.org/10.1190/1.1567214.

Urbancic, T. I., and S. C. Maxwell, 2002, Source parameters of hydraulic fracture induced microseismicity: Presented at the SPE Annual Technical Conference and Exhibition, Society of Petroleum Engineers.

Warpinski, N., 2009, Microseismic monitoring: Inside and out: Journal of Petroleum Technology, **61**, 80–85, http://dx.doi.org/10.2118/118537-JPT.

Yilmaz, O., 2001, Seismic data analysis: Society of exploration geophysicists.

Zhang, Z., J. W. Rector, and M. J. Nava, 2015, Improving microseismic event location accuracy with head wave arrival time: Case study using Marcellus shale: 85th Annual International Meeting, SEG, Expanded Abstracts, http://dx.doi.org/10.1190/segam2015-5919420.1.

Zimmer, U., 2011, Microseismic design studies: Geophysics, **76**, no. 6, WC17–WC25, http://dx.doi.org/10.1190/geo2011-0004.1.